

Analysis of cooling of the exhaust system in a small airplane by applying the ejector effect

Łukasz Złoty*, Piotr Łapka, Piotr Furmański

Institute of Heat Engineering, Warsaw University of Technology, Poland

Abstract

This paper presents a thermal analysis of elements of the exhaust system of the redesigned airplane I-23. In order to improve the thermal performance of the exhaust system and decrease thermal loads inside the engine bay, modifications of the initial geometry of the cover pipe were proposed. This pipe shields the nacelle interior from thermal interaction and direct contact with the hot exhaust pipe. Several openings were created in its wall to increase the mass flow rate of the cold air sucked in from the nacelle interior to the gap between the exhaust pipe and its cover due to the ejector effect. Then numerical models were developed and simulations for flight conditions were carried out for the original and modified exhaust systems. The results obtained for both geometries were compared, showing that openings in the cover duct resulted in a high mass flow rate flowing through the gap between exhaust pipe and its cover and a lower exhaust pipe temperature. Even though the number, locations and cross-section area of the openings were selected arbitrarily, better thermal performance was obtained for the modified exhaust system.

Keywords: exhaust system, heat transfer, numerical simulation, thermal model,

1. Introduction

Good design of airplane propulsion systems is important for multiple reasons. Many different analyses of its elements, e.g., safety, structural and thermal, should be carried before the first flight. Moreover, optimizations of power unit systems are needed to improve airplane performance. Similar investigations were performed for selected elements of the engine system of the recently redeveloped airplane I-23 [1–6]. In the new conception, the I-23 in the tractor configuration is equipped with a turboprop engine located in the fuselage. The exhaust gases at temperatures reaching almost 650°C are removed through the exhaust system, which is partially located inside the engine bay. Therefore the exhaust pipe may thermally interact with the nacelle interior and other systems located close to it. Poor design of the exhaust system may lead to the worst-case scenario of thermal damage to the cowling or devices located inside the nacelle. In previous studies [1, 4] temperature hot spots on the inner side of the nacelle cover were observed due to thermal radiative heat transfer between the hot engine and exhaust system surfaces and the cowling. Fortunately, the temperature peaks

were below the maximum allowable temperature of operation of the composite materials used to make the cover. However, these results do not provide total comfort that no thermal damage will happen to the cowling or engine systems. Therefore, there is a still need to improve airplane safety and performance, e.g., by decreasing the temperature of the exhaust system and its direct and indirect thermal interaction with the nacelle and systems located in the engine bay.

In this paper elements of the exhaust system of the I-23, i.e., the exhaust pipe and its cover were investigated and initially optimized by means of the CFD technique, which deals with various types of heat and fluid flow problems [7–9]. In order to improve the thermal performance of the exhaust system, a modification of its geometry was proposed. Several openings were arbitrarily created in the cover duct wall. The role of the holes was to increase the mass flow rate of the cold air sucked in from the nacelle interior to the gap between the exhaust pipe and its cover due to the ejector effect. The higher mass flow rate of the cold air was expected to decrease the temperatures of the exhaust pipe and the cover and reduce thermal loads inside the engine bay. Moreover, this action would be beneficial to the safety of the airplane. In order to investigate the performance of both the original and modified exhaust systems, ANSYS CFD software was used to develop numerical models of the exhaust systems. Then

*Corresponding author

Email addresses: lukasz.zloty@itc.pw.edu.pl (Łukasz Złoty),

Piotr.Lapka@itc.pw.edu.pl (Piotr Łapka),

piotr.furmanski@itc.pw.edu.pl (Piotr Furmański)

thermo-fluid simulations for flight conditions were performed and the results obtained for both geometries were compared.

2. Original and modified geometries of the exhaust system

The geometries analyzed in the paper were based on the shapes and dimensions of the newly redeveloped turboprop airplane I-23 [1–6], which is shown in Fig. 1 A with detailed views of the front part of the nacelle and the engine bay—Fig. 1 B and C. The newly developed exhaust system consists of the exhaust pipe and cover ducts which shield the nacelle interior from direct contact with hot surfaces and thermal radiation given off by the hot exhaust pipe. Due to the ejector effect the gaps located between the exhaust pipe and its covers become efficient air outlets from the nacelle interior to the surroundings. Therefore they are also considered as parts of the engine bay ventilation system. Additionally, the air flowing through these gaps cools down the exhaust pipe and the covers, reducing thermal loads inside the nacelle.

In this work the developed geometrical model reflected to some extent the real shape of the newly redesigned engine bay and exhaust system of the airplane I-23. Due to the symmetry of the computational domain, the limited computational resources at hand and noting the wish to have a reasonable time of simulation, only the front part of the engine bay interior was modeled, including part of the engine and nacelle, exhaust pipe and cover ducts—see Fig. 2. The zone which accounts for the surroundings of the plane was created outside the nacelle in such a way that the external air flow can be simulated. The developed geometrical model is presented in Fig. 2. The whole length of the computational domain was 1.8 m, the height 1.0 m and the width 1.26 m.

In order to check the possibility of improving the performance of the nacelle ventilation systems and decreasing the temperature of the exhaust system, modifications were made to the exhaust pipe covers. Eleven holes were made in each external duct, as shown in Fig. 3. The locations, number and cross-sectional area were selected arbitrarily. It is believed that these holes improve the air mass flow rate flowing from the nacelle interior through gaps between the exhaust pipe and the covers to the surroundings. Moreover, the higher air mass flow rate should result in a decrease in the respective temperature of the exhaust pipe and the covers. Weaker thermal interactions of the exhaust system with the nacelle interior should be observed for the modified geometry.

3. Mathematical model

The air flow inside and outside the nacelle was assumed to be incompressible and turbulent. Moreover, the influence of propeller rotation on flow patterns was neglected. The steady state form of the Reynolds averaged incompressible continuity and momentum equations were assumed as follows:

$$\frac{\partial u_j}{\partial x_j} = 0 \quad (1)$$

$$\rho \frac{\partial(u_i u_j)}{\partial x_j} = -\frac{\partial p}{\partial x_i} + \frac{\partial}{\partial x_j} \left[\mu \left(\frac{\partial u_i}{\partial x_j} + \frac{\partial u_j}{\partial x_i} \right) - \overline{\rho u'_i u'_j} \right] \quad (2)$$

where: u and u' are the mean and fluctuating velocity components, respectively, p is the pressure, μ is the dynamic viscosity and ρ is the density. The Reynolds stress tensor was modeled via the turbulence model, employing the Boussinesq hypothesis:

$$-\overline{\rho u'_i u'_j} = \mu_t \left(\frac{\partial u_i}{\partial x_j} + \frac{\partial u_j}{\partial x_i} \right) - \frac{2}{3} \rho k \delta_{ij} \quad (3)$$

where: δ is the Dirac delta function, μ_t is the turbulent (eddy) viscosity, k is the turbulent kinetic energy.

The turbulence was modeled with the realizable $k - \epsilon$ model [10]. The transport equations for k (turbulent kinetic energy) and ϵ (turbulent dissipation rate) were used in the following form:

$$\frac{\partial(\rho k u_j)}{\partial x_j} = \frac{\partial}{\partial x_j} \left[\left(\mu + \frac{\mu_t}{\sigma_k} \right) \frac{\partial k}{\partial x_j} \right] + G_k - \rho \epsilon \quad (4)$$

$$\frac{\partial(\rho \epsilon u_j)}{\partial x_j} = \frac{\partial}{\partial x_j} \left[\left(\mu + \frac{\mu_t}{\sigma_\epsilon} \right) \frac{\partial \epsilon}{\partial x_j} \right] + \rho C_1 S \epsilon - \rho C_2 \frac{\epsilon^2}{k + \sqrt{\nu \epsilon}} \quad (5)$$

where: G_k represents the generation of turbulent kinetic energy due to the mean velocity gradients, S and C_1 are the model variables, C_2 is model constants, ν is the kinematic viscosity, σ_k and σ_ϵ are the turbulent Prandtl numbers for k and ϵ , respectively. In the realizable $k-\epsilon$ model turbulent viscosity is given by $\mu_t = \rho C_\mu k^2 / \epsilon$ where C_μ is the model variable. For more details see Versteeg and Malalasekera [10]. The realizable $k - \epsilon$ model was applied with the scalable wall function approximation, which avoids the deterioration of the solution under grid refinement close to the solid boundary below $y^+ < 30$, where y^+ is a dimensionless distance from the wall to the first mesh node.

Considering the air filling the computational domain to be transparent to thermal radiation, the energy equation for incompressible turbulent flow in the steady state can be written in the following form:

$$u_j c_p \frac{\partial T}{\partial x_j} = \frac{\partial}{\partial x_j} \left[(\lambda + \lambda_t) \frac{\partial T}{\partial x_j} \right] \quad (6)$$

where: T is temperature, λ is the molecular thermal conductivity, λ_t is the turbulent thermal conductivity ($\lambda_t = c_p \mu_t / Pr_t$), c_p is the specific heat and Pr_t is the turbulent Prandtl number (the default value $Pr_t = 0.85$ was assumed).

Inside the engine bay the radiative heat transfer was assumed to occur only between gray opaque surfaces, which were assumed to be diffusely emitting and reflecting thermal radiation. The emitted radiation intensity at the surface (I_w) for $\mathbf{s} \cdot \mathbf{n}_w > 0$ was given by [11–13]:

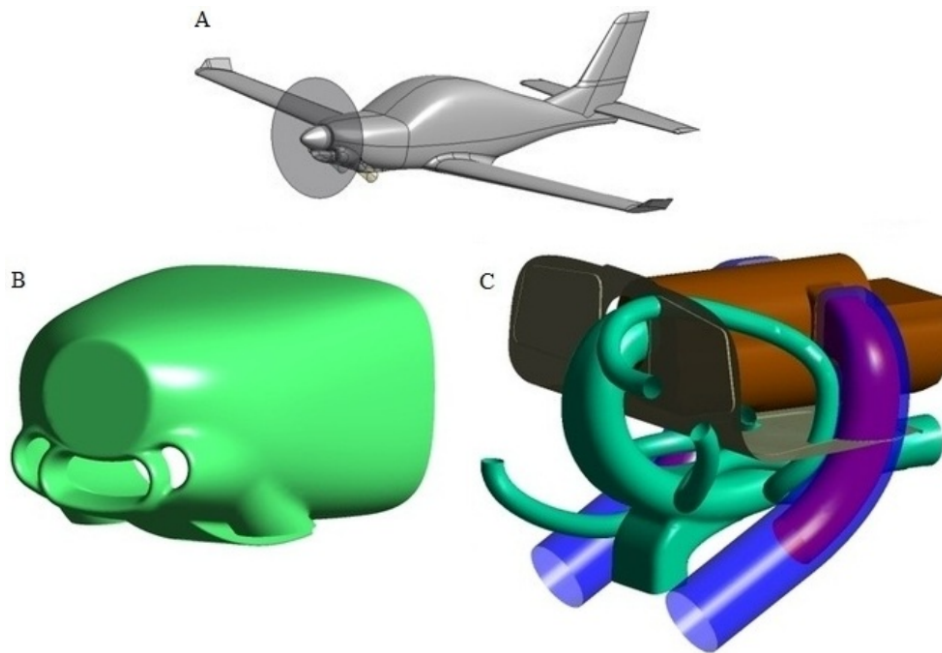


Figure 1: View of: A) the newly redeveloped airplane I-23, B) the front part of the nacelle, C) the engine bay

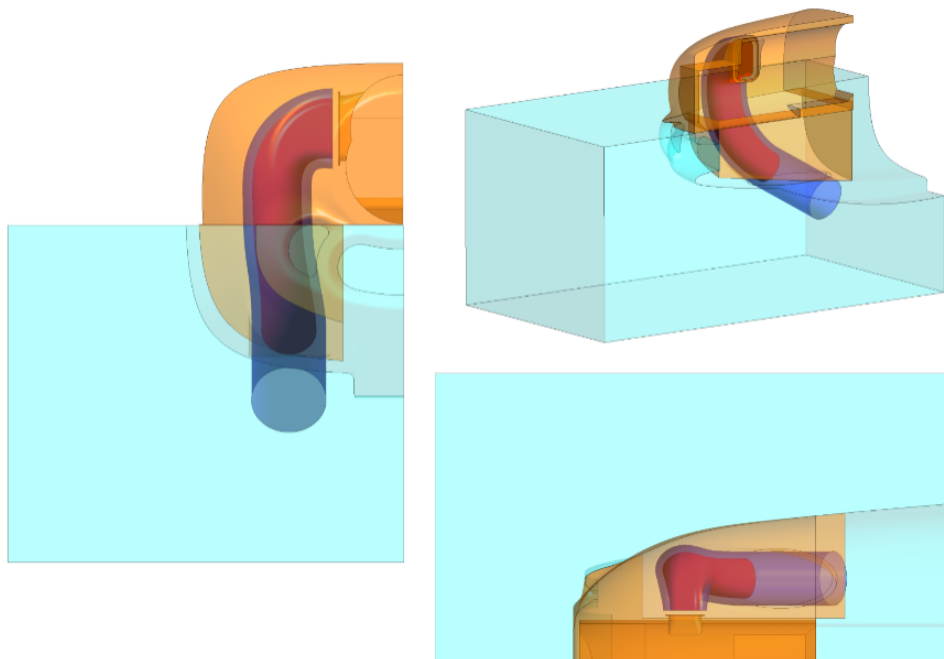


Figure 2: Views of the geometrical model (light blue zone—the external air domain, orange zone—the internal air domain)

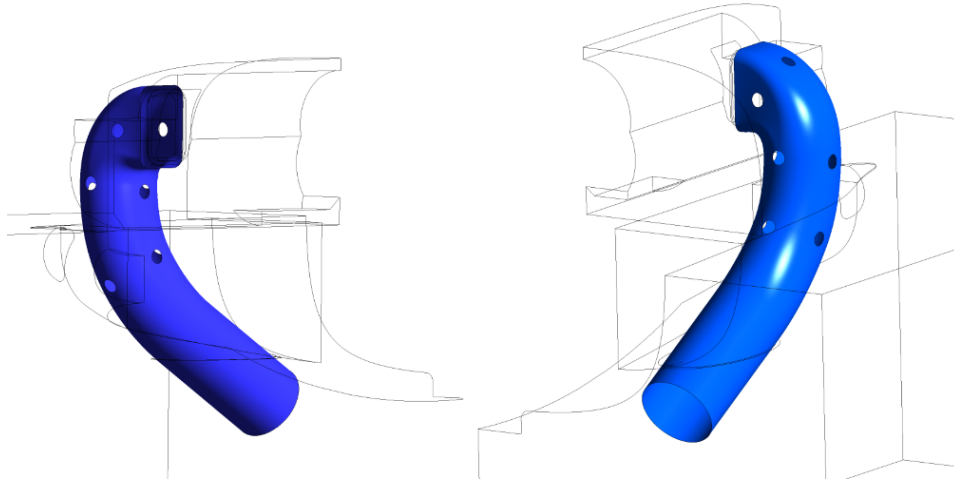


Figure 3: Views of the modified external cover duct

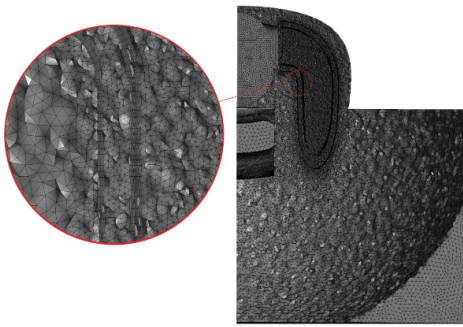


Figure 4: View of the mesh details

$$I_w = \frac{\epsilon_w \sigma T_w^4}{\pi} + \frac{1 - \epsilon_w}{\pi} \int_{s \cdot n_w < 0} I |s \cdot n_w| d\Omega \quad (7)$$

where: I is the incident radiation intensity, \mathbf{n}_w is the wall normal vector, \mathbf{s} is the radiation direction vector, T_w is the surface temperature, ϵ_w is its emissivity, Ω stands for the solid angle and the symbol σ denotes the blackbody constant.

4. Numerical model

The fluid domains for the original (case I) and modified (case II) geometries were discretized using the hybrid mesh (Fig. 4). Moreover, the inflation layers of structured elements were generated close to the walls of the exhaust pipe and its cover (Fig. 4). In the rest of the fluid domain grids were unstructured. In both cases the meshes contained tetrahedral and prism elements. The meshes were also denser near parts of stronger curvature. Both meshes for cases I and II consisted of about 12 m of elements. Their qualities were within an acceptable range, e.g., the maximum aspect ratio and skewness were below 45 and 0.9, respectively.

Following boundary conditions were assumed during simulations:

1. The mass flow rates of 54.737 kg/s and 0.750 kg/s for inlets at the front surface of the surrounding air domain and at the exhaust pipe, respectively.
2. The pressure outlet at the top, bottom, side and back surfaces of the surrounding air domain, at air inlets in the nacelle mouth (see [1, 2, 4, 5]) and at all virtual surfaces limiting the fluid domain enclosed by the nacelle. To control the mass flow rates flowing through nacelle mouth inlets, target mass flow rate options were applied as described in [1, 4].
3. Stationary walls at the nacelle and engine surfaces.
4. Symmetry at all surfaces in the middle cross-section of the system.

Calculations were made for the airplane's cruising speed of 255 km/h at an altitude of 3000 m. For these flight conditions the ambient air parameters and properties were estimated from the International Standard Atmosphere Model [14], i.e., the ambient air temperature and pressure were 268.65 K and 70108.5 Pa, respectively—see [1]. The inlet temperature of the exhaust gases was set at 923 K. The engine walls were kept at 373 K, while the nacelle surfaces were assumed adiabatic. The 1D shell conduction model was applied to account for materials and thicknesses of the exhaust pipe and its covers (1 mm steel ducts). Moreover, emissivities of all metallic and nacelle surfaces were equal to 0.6 and 0.9, respectively. More details about assumed boundary conditions may be found in [1, 4, 5].

The problem was solved applying the pseudo-transient solver. Thermal radiation was modeled with the Finite Volume Method for radiative heat transfer [12, 13] with angular discretization and pixelation at the levels of 2×4 and 5×5 , respectively. Additionally, the second order upwind and PRESTO! schemes were applied to all balance and pressure

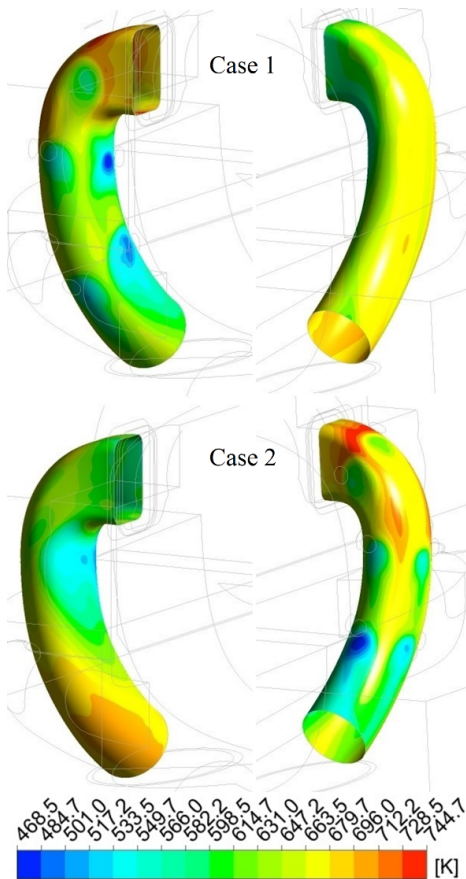


Figure 5: Temperature distributions on the exhaust pipe for the original (case 1) and modified (case 2) geometries

correction equations, respectively. All calculations were performed using the Finite Volume Method [10] based software ANSYS Fluent 15.0.

5. Results and discussion

Temperature distributions on the exhaust pipe and its cover for both analyses cases (cases 1 and 2) are shown in Fig. 5 and 6, respectively. The proposed changes in the geometry of the external cover duct have a significant influence on the exhaust pipe surface temperature distribution (Fig. 5). Lower temperatures for the modified geometry than for the original one can be perceived in the middle and rear parts of the exhaust pipe. In several locations, e.g., opposite holes in the cover a decrease in temperature greater than 100 K is observed. This behavior is a result of higher mass flow rates of the cold air flowing in these regions, which increase the convective heat rate from the hot exhaust pipe. In the former part of the exhaust system the temperature of the exhaust pipe is higher for the modified geometry than for the original one. This behavior is a result of a drop in the mass flow rate sucked in from the nacelle to the gap between the exhaust pipe and its cover. Lower mass flow rate in this region is

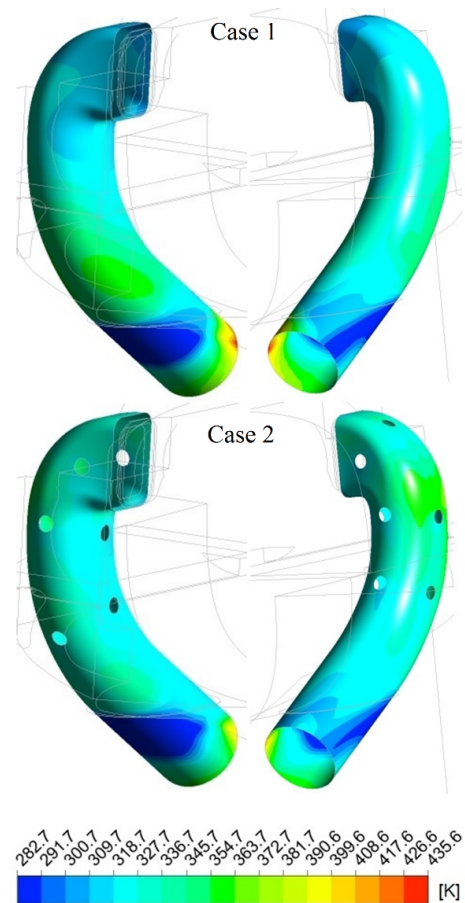


Figure 6: Temperature distributions on the cover pipe for the original (case 1) and modified (case 2) geometries

responsible for the lower convective heat rate and higher exhaust pipe temperature. The deterioration in the mass flow rate flowing between tubes in the former part of the exhaust system is related to additional air paths through holes in the middle and rear parts of the cover tube. The averaged exhaust pipe temperatures were 642.4 K and 620.9 K for the original and modified geometry, respectively. These values refer to a 3.3% decrease in the exhaust pipe averaged temperature.

Similar temperature behavior is observed on the cover pipe (Fig. 6), i.e., with the modified geometry the temperature increases in the former part, while there are drops in the middle and rear parts as well as close to openings. The averaged exhaust pipe cover temperatures were almost the same for both cases, i.e., 333.4 K and 329.7 K for the original and modified geometry, respectively.

Moreover, the mass flow rates flowing in the gap between the exhaust pipe and its cover due to the ejector effect were also analyzed. The value of the mass flow rate increased by about 20% from 0.313 kg/s to 0.376 kg/s for the original and modified geometries, respectively.

6. Conclusions

The paper presents thermo-fluid analyses of part of the exhaust system of the recently redeveloped airplane I-23 in the tractor configuration with one engine in the fuselage. The cover duct, which shields the nacelle interior from direct and indirect contact with the hot exhaust pipe, was modified to lower exhaust system temperatures. Several openings were created in the cover wall which were expected to increase the mass flow rate of the cold air sucked in from the nacelle interior to the gap between exhaust pipe and its cover due to the ejector effect. The higher mass flow rate of the cold air in the gap was to decrease the exhaust and cover pipe temperatures and reduce thermal loads inside the engine bay.

In order to check the performance of the new conception of the exhaust system, numerical models of the original and modified exhaust systems were developed using ANSYS CFD software. Then thermo-fluid simulations were performed for the flight conditions and a comparison made of the results obtained.

The mass flow rate of the cold air sucked into the gap between the exhaust pipe and the cover increased by about 20% for the modified geometry and the average exhaust pipe temperature dropped by 21.5 K. However in some regions the temperature of the exhaust pipe dropped by more than 100 K. Moreover, a deterioration of heat transfer conditions were observed in the former part of the exhaust pipe due to lower mass flow rate flowing there. The averaged cover pipe temperature remained the same for both analyzed geometries.

The studies presented in this paper showed one of the possible ways to increase the thermal performance of the exhaust system and decrease thermal loads inside the nacelle. Even though the number, locations and cross-section area of openings were selected arbitrarily, a rise in the cold air mass flow rate in the gap and a drop in the averaged exhaust pipe temperature were obtained. Optimization of the number, locations and cross-section area of the openings should lead to even better results.

References

- [1] P. Łapka, M. Seredyński, P. Furmański, A. Dziubiński, J. Banaszek, Simplified thermo-fluid model of an engine cowling in a small airplane, *Aircraft Engineering and Aerospace Technology: An International Journal* 86 (3) (2014) 242–249.
- [2] W. Stalewski, J. Żółtak, The preliminary design of the air-intake system and the nacelle in the small aircraft-engine integration process, *Aircraft Engineering and Aerospace Technology: An International Journal* 86 (3) (2014) 250–258.
- [3] T. Goetzendorf-Grabowski, Formulation of the optimization problem for engine mount design–tractor propeller case, *Aircraft Engineering and Aerospace Technology: An International Journal* 86 (3) (2014) 228–233.
- [4] P. Łapka, M. Bakker, P. Furmański, H. van Tongeren, Comparison of 1d and 3d thermal models of the nacelle ventilation system in a small airplane, *Aircraft Engineering and Aerospace Technology* 90 (1) (2018) 114–125.
- [5] P. Łapka, M. Seredyński, P. Furmanski, Investigation of thermal interactions between the exhaust jet and airplane skin in small aircrafts, *Progress in Computational Fluid Dynamics 2017*, in print. 90 (1) (2017) 114–125.
- [6] A. Iwaniuk, W. Wiśniowski, J. Żółtak, Multi-disciplinary optimisation approach for a light turboprop aircraft-engine integration and improvement, *Aircraft Engineering and Aerospace Technology: An International Journal* 88 (2) (2016) 348–355.
- [7] J. Polewka, P. Krawczyk, P. Prusiński, Cfd modelling of low-emission pulverized coal swirl burner, *Journal of Power Technologies* 96.
- [8] W. Smuga, L. J. Kapusta, A. Teodorczyk, Numerical simulations of n-heptane spray in high pressure and temperature environments, *Journal of Power Technologies* 97 (1) (2017) 1.
- [9] M. Chmielewski, M. Gieras, Planck mean absorption coefficients of h₂o, co₂, co and no for radiation numerical modeling in combustions flows, *Journal of Power Technologies* 95 (2) (2015) 97.
- [10] H. K. Versteeg, W. Malalasekera, *An introduction to computational fluid dynamics: the finite volume method*, Pearson Education, 2007.
- [11] J. R. Howell, R. Siegel, M. Menguc, *Thermal radiation heat transfer*, CRC press, 1992.
- [12] P. Łapka, P. Furmański, Fixed grid simulation of radiation-conduction dominated solidification process, *Journal of Heat Transfer* 132 (2) (2010) 023504.
- [13] P. Łapka, P. Furmański, Fixed cartesian grid based numerical model for solidification process of semi-transparent materials I: modelling and verification, *International Journal of Heat and Mass Transfer* 55 (19-20) (2012) 4941–4952.
- [14] International Standard Atmosphere Model <http://www.aerospacweb.org/design/scripts/atmosphere/>, 2017.